The Journal of Neuroscience, October 1988, 8(10): 3770–3784

Effect of Testosterone on Input Received by an Identified Neuron Type of the Canary Song System: A Golgi/Electron Microscopy/ Degeneration Study

R. A. Canady,[1] G. D. Burd,[2] T. J. DeVoogd,[3] and F. Nottebohm[1]

[1]The Rockefeller University, New York, New York 10021, [2]Department of Molecular and Cellular Biology, University of Arizona, Tucson, Arizona 85721, and [3]Department of Psychology, Cornell University, Ithaca, New York 14853

Combinations of the Golgi stain, anterograde degeneration, and electron microscopy are used to further characterize the hormone-sensitive "type IV" neuron of the forebrain nucleus robustus archistriatalis (RA) of adult female canaries. Anterograde degeneration was used to "stain," at the electron-microscopic level, the axon terminals of neurons projecting to RA from hyperstriatum ventralis, pars caudalis (HVc) and from the lateral magnocellular nucleus of the anterior neostriatum (L-MAN). The HVc neurons projecting to RA type IV cells form synapses predominantly on the dendritic spines of those cells, while L-MAN neurons that project to RA type IV cells form a 2.5:1 mixture of shaft and spine synapses. There were about 1000 synapses from HVc neurons (about 30% of all spine synapses) on typical type IV cells and about 50 synapses from L-MAN neurons.

Earlier work had shown that in female canaries the dendrites of type IV neurons of the avian song control nucleus RA increase in total length after systemic testosterone treatment, and that this increase in dendritic length was accompanied by the development of malelike song. We now show that testosterone treatment also increases the number of dendritic spines present in type IV neurons. Presumably this is accompanied by an increase in the number of synaptic inputs received by type IV cells.

Earlier evidence suggested that the testosterone-induced addition of extra dendritic length to type IV cells occurred at existing dendritic tips. We tested the hypothesis that these added peripheral ends received a special subset of inputs, which might then account for the change in behavior, and found it to be false. Mapping and counts of degenerating synapses resulting from lesion of HVc and L-MAN suggest that under the influence of hormone, new synapses are added throughout the dendritic tree, with no special distribution or change in ratio of inputs occurring at the tip of dendrites. Under the influence of testosterone, each type IV cell may receive only "more of the same" inputs it received before onset of treatment. We speculate on how such changes in circuitry may relate to song stability and learning.

Received Sept. 8, 1987; revised Feb. 1, 1988; accepted Feb. 8, 1988.

We thank Dr. David Vicario for his comments on the manuscript. This research was supported by National Research Service Award Predoctoral Training Grant 5-T32 GMO7524, the Whitehall Foundation, and PHS Grant NS 17991.

Correspondence should be addressed to Fernando Nottebohm, Box 137, The Rockefeller University, 1230 York Avenue, New York, NY, 10021.

Canaries, like many other songbirds, learn their song by reference to auditory information (Marler and Waser, 1977; Waser and Marler, 1977). Brain pathways for the control of this behavior have been described. They consist of anatomically discrete nuclei (Fig. 1). The hyperstriatum ventralis, pars caudalis (HVc) projects to the nucleus robustus archistriatalis (RA), which, in turn, projects to the hypoglossal motorneurons that innervate the trachea and syrinx (nXIIts) (Nottebohm et al., 1976). RA also receives input from the lateral division of the magnocellular nucleus of the anterior neostriatum (L-MAN) (Nottebohm et al., 1982), which has been shown to be important for song learning in zebra finches (Bottjer et al., 1984). HVc, RA and nXIIts have been shown to be sexually dimorphic. These nuclei are larger in males, which sing a lot and develop complex songs, than in females, which sing infrequently, if at all (Nottebohm and Arnold, 1976).

The present study focuses on the "type IV" class of neuron in nucleus RA (Fig. 2), henceforth referred to as type IV neurons. This is the most commonly stained RA neuron when the Golgi impregnation method is used. It is characterized by spiny dendrites that branch repeatedly and distribute themselves in all directions around the soma; these dendrites are longer in adult male than in adult female canaries (DeVoogd and Nottebohm, 1981a).

Female canaries that were ovariectomized soon after hatching and treated with testosterone at 1 year of age develop malelike song; this is associated with a 90% increase in HVc size and a 53% increase in RA size (Nottebohm, 1980). This treatment induces a 49% increase in the length of the dendrites of type IV neurons (DeVoogd and Nottebohm, 1981b). The increase in dendritic length is accompanied by a 51% increase in the number of synapses present in RA (DeVoogd et al., 1985). Two-year-old female canaries with intact ovaries also respond to testosterone, in this case with a 69% increase in RA volume (Nottebohm, 1980).

The above findings have increased our interest in type IV neurons. Where do they project to? (This is the theme of a separate study.) What kinds of inputs do they receive? Is the kind of input and distribution affected by testosterone treatment? The latter 2 questions, addressed here, are relevant not only to our better understanding of the song control system of songbirds, but are also of interest in probing the kinds of circuitry changes that can be induced by hormones. We therefore used Golgi staining to clearly identify type IV neurons, together with electron microscopy and lesioning, to trace connectivity with ultrastructural degeneration. A second variable was the

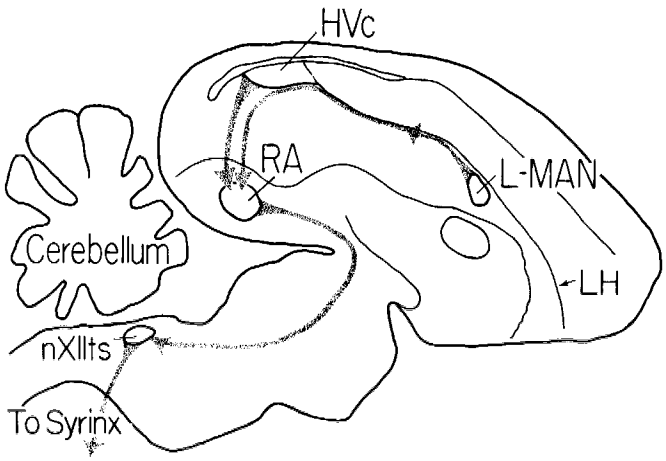

Figure 1. Sagittal view of the avian brain showing the projections from L-MAN and HVc to RA and the path that the type IV neurons of RA follow to reach the motor neurons controlling the syrinx.

presence or absence of testosterone, known to cause synaptogenesis in this system.

Materials and Methods

Animals and hormone treatment. All canaries used were taken from the Rockefeller University Field Research Center Belgian Waserschlager colony. A total of 24 female canaries were processed for Golgi/electron-microscopic analysis of inputs to type IV dendrites. These animals were implanted with hormone capsules in late April and the beginning of May and lesioned in late May and the beginning of June. They were between 20 and 24 months old at time of implantation and had had breeding experience the year previous. The implanted females were isolated singly in separate cages during the month of hormone treatment. The unimplanted females used were left in breeding pairs until about 2 d prior to the time of lesioning. To determine the concentration of degenerating synapses in RA resulting from lesion of HVc and L-MAN, unilateral lesions were made of L-MAN in 8 untreated females (4 used) and 5 testosterone-treated females (5 used), and HVc in 7 untreated females (5 used) and 6 testosterone-treated females (3 used).

Testosterone propionate in silastic capsules (5 mm packed hormone; I.D. of capsule, 0.03 in.; O.D., 0.065 in.) was implanted subcutaneously during the month of May, according to the method of Legan et al. (1975). Such implants have been shown to induce plasma testosterone levels in ovariectomized female canaries comparable to those in unpaired males in reproductive condition (compare Luine et al., 1980, and Nottebohm et al., 1987). This kind of implant has also been shown to induce malelike song in adult female canaries and to promote hypertrophic changes in the anatomy of their song-control circuits (Nottebohm, 1980; DeVoogd and Nottebohm, 1981b). The animals were lesioned 1 month after hormone implantation. The testosterone-implanted females used in this study were monitored to ensure that they all developed the loud, persistent, and stereotyped song typical of adult males in reproductive condition. The unimplanted females were not monitored; we know from other observations that female song does not occur during this time of year.

The volume of nucleus RA was expected to be larger in females treated with testosterone than in untreated females (Nottebohm, 1980). In the present study, volume was estimated from the Golgi-stained sections. Brains in which stain artifact obscured the boundaries of RA were rejected for volume reconstruction. Eight untreated females and 9 testosterone-treated females were used for volume estimation.

Lesions. In each subject, either nucleus L-MAN or HVc was destroyed unilaterally (left side only) by electrolytic lesion in order to selectively "stain" their terminal boutons in nucleus RA. A total of 24 canaries were lesioned and processed for Golgi/electron-microscopic analysis, and 16 more were lesioned and processed for electron microscopy alone to determine the time course of synaptic degeneration. Insect pins ("00"), coated except at their tips with Insulex, were advanced stereotactically into the brain, while the animal was under Chloropent anesthesia, to the coordinates AP +4.2, ML 1.4, DV 2.4 for L-MAN and AP 0.0, ML 2.8, DV 0.4 for HVc (using the atlas of Stokes et al., 1974). A local anesthetic (Xylocaine) was used around the wound. The ground lead was placed under the skin near neck muscles that are exposed in the course of surgery, and direct anodal current of 70 μA was then passed for approximately 60 sec. Several lesions were made in a cluster centered on the above coordinates to be sure of destroying the entire nucleus. The head wound was closed with collodion and the animals were allowed to recover from anesthesia. They were then kept in isolation until they were killed.

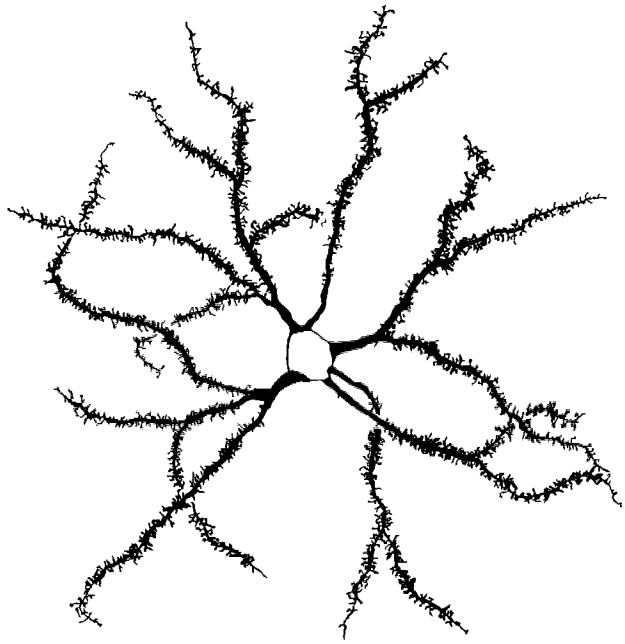

Figure 2. Camera lucida drawing of a gold-toned, Golgi-stained RA type IV neuron of an untreated female. In gold-toned preparations, the cell body is transparent. Bar, 20 μm.

The lesions were confirmed in all cases by examining the lesion site in Nissl-stained material. In the brains with L-MAN lesions, the rostral half of the brain (RA is in the caudal half) was sectioned at 70 μm using a Vibratome. The sections were mounted on glass slides and stained with cresyl violet. In brains with HVc lesions, the dorsal 2 mm of the caudal half of the brains was removed using a tissue chopper, leaving the ventral part of the brain containing RA free for Golgi staining. The 2-mm-thick slab containing the HVc lesion was then embedded in gelatin/albumin, sectioned frozen at 70 μm on a sliding microtome, and stained with cresyl violet.

Since the boundaries of the nuclei that were lesioned are well defined, the determination as to whether the nuclei were completely destroyed was straightforward and unambiguous. If any portion of the nucleus to be lesioned was still present in Nissl-stained sections of the lesion site, the subject was rejected.

L-MAN fiber damage when lesioning HVc. Since the projection from L-MAN to RA passes just lateral and ventral to HVc (Nottebohm et al., 1982) large lesions that were intended to hit HVc may also have damaged L-MAN fibers. Unfortunately, kainic acid lesions of HVc made in 9 canaries in an attempt to avoid damage to fibers of passage from L-MAN produced an unsatisfactory amount of degeneration compared to electrolytic lesions and poor tissue morphology at the electron-microscopic level in RA. Thus, it was necessary to electrolytically lesion HVc while trying to avoid the fibers of passage coming from L-MAN. This was done by careful placement of the lesions and rejection of those subjects in which the lesions did not completely destroy the cells of HVc or extended too far into the area just lateral and ventral to HVc, where the L-MAN fibers were known to course. In spite of these considerations, it is likely that at least some fibers coursing from L-MAN to RA were damaged. However the error resulting from such damage was likely to be small. On the basis of a comparison of the concentration

of degenerating boutons on RA type IV cells resulting from HVc lesions and L-MAN lesions in many animals, HVc boutons outnumber those from L-MAN in RA by 20 to 1. Therefore even if the fibers from L-MAN were completely severed in HVc-lesioned material used to estimate synapse concentration, the resulting overestimation of HVc synapses in RA would not exceed 5%.

Nucleus L-MAN, on the other hand, is well isolated from other nuclei or fiber pathways synapsing in RA. Therefore, large lesions encompassing it and the tissue directly surrounding it are no different from smaller lesions restricted exclusively to L-MAN in terms of the type and quantity of terminals caused to degenerate in RA for the survival times used. For this reason, large lesions were used to ensure that L-MAN was completely destroyed in all animals.

Survival time for degeneration. Lesion-induced degeneration was used to "stain" synapses from a given source occurring in RA. The darkness of a profile is an indication of the stages of degeneration. Initially, degenerating boutons appear slightly darker than unaffected synapses, and vesicles and the presynaptic densities are still easily distinguished. However, as degeneration proceeds, the boutons become darker and smaller and synaptic constituents are less evident. Eventually the degenerating structures are engulfed and disappear (see Peters and Feldman, 1976).

An appropriate survival time for dendrite mapping was determined using a total of 16 L-MAN-lesioned untreated and testosterone-treated females with survival times ranging from 1 to 7 d. By 1 d after the first appearance of degenerating synapses, the range of darkness of degenerating synapses was found to be small. That is, a homogeneous population of darkened synapses was observed at this survival time and could be unambiguously distinguished from nondegenerating synapses. The number of degenerating profiles occurring in a 3000 μm^2 area of central RA was counted at each survival time. While the number of animals at each survival time was too small to yield an accurate estimate of the concentration of degenerating synaptic profiles, the concentration value appeared to reach a plateau 1 d after the first appearance of recognizably degenerating profiles and then to decline 3–4 d later. These results suggest that a focused wave of degeneration occurs at a given time after lesioning. Thus, 1 d after the first appearance of darkened degenerating profiles was chosen as the optimal time for observing degenerating synapses in this material. In untreated female canaries, presynaptic boutons begin darkening approximately 2 d following lesion of HVc and 3 d following lesion of L-MAN.

An unexpected effect of testosterone on the survival time that produced optimal degeneration after L-MAN lesions was observed in RA. Initial pilot studies to determine the optimal survival time for observing the degenerating boutons were done with untreated females. The distance from lesion sites to RA in males and in testosterone-treated or untreated females is essentially the same, so no difference in survival time due to hormonal manipulation was expected. However, the hormone manipulation did have an effect on the time it took to begin seeing osmiophilic degenerative changes in the synapses from L-MAN. Figure 3 shows the appearance of degenerating L-MAN synapses in RA at 72 hr survival in an untreated female and 107 hr in a testosterone-treated female. As can be seen, a 72 hr survival time in an untreated female produces dark, degenerating profiles in which vesicles cannot be seen (Fig. 3*B*), while a longer survival time in a testosterone-treated female produces degeneration that appears to be of an earlier stage (Fig. 3*A*, lighter shade, with vesicles and presynaptic thickening visible). Degenerating terminals were not seen in testosterone-treated females at 72 hr survival after L-MAN lesion, and in fact were not seen with survival times of less than 90 hr. In normal male canaries, presumed to have higher testosterone levels than untreated females, the survival time when degenerating terminals first start appearing in RA after L-MAN lesions was also greater than 90 hr. This effect of testosterone treatment was not observed for synapses resulting from lesions of HVc.

Therefore, survival times used to ascertain concentrations of synapses per unit volume and to map the positions of degenerating terminals on identified neurons were set differentially on the basis of these pilot data. Those times were 60 hr for lesions of HVc, 80 hr for lesions of L-MAN in untreated females, and 110 hr for lesions of L-MAN in testosterone-treated female canaries.

Golgi-staining procedure. In order to achieve optimal ultrastructural preservation of tissue, the Golgi-staining method of Freund and Somogyi (1983) was used. The brains were perfused with sodium phosphate-buffered 1.0% paraformaldehyde and 1.25% glutaraldehyde fixative, left in the skulls overnight, blocked at A–P +1.0 (using the atlas of Stokes et al., 1974), and excised into fresh fixative for 4–6 hr. After removing portions containing lesion sites for separate processing, the remaining tissue containing RA was sectioned with a Vibratome at 140 μm intervals, osmicated using 1% OsO_4 in buffer for 1 hr, and stacked to reform the shape of the original block. The stack was covered with a 7% solution of agar and Golgi-stained using a double-impregnation procedure consisting of 7 d in 2.5% potassium dichromate and 2 d in 1% silver nitrate, repeated. After Golgi staining the agar-coated stacks were placed in ascending concentrations of glycerin and then stored in 100% glycerin. The method used to prepare the Golgi-impregnated cells for electron-microscopic analysis was basically that of Fairen et al. (1977). The Golgi-stained sections, still in glycerin, were exposed to light in a cold room overnight. Sections were placed in descending concentrations of Ag-Cr_2O_7-saturated glycerin to distilled water, then placed for 15–60 min in 0.05% $AuCl_4$, distilled water, 0.05% oxalic acid for 2 min, rinsed in distilled water and 1% $Na_2S_2O_3$ for 60 min. The tissue was dehydrated through an ascending series of ethanol concentrations (50, 70, 95, and 100%; at the 70% ethanol wash the Golgi tissue was block-stained for electron microscopy with 1% uranyl acetate in 70% ethanol for 60 min). The tissue was then washed with propylene oxide and embedded in Epon between Teflon-coated coverslips.

For thin-sectioning the Teflon coverslips were removed from the tissue and appropriate areas of tissue dissected out of the flat-embedded section. These small plastic chips of tissue were then glued to blank blocks of cured Epon with cyanoacrylate and trimmed down either to the borders of RA or to the sphere encompassed by a single Golgi-stained cell. This was facilitated with microscopic examination of the tissue using light transmitted through the block.

Spine counts. Spine counts were done using 1200× final magnification on dendritic "paths" that were chosen from coded tissue that had been prepared for Golgi/electron-microscopic analysis. A dendritic path began at the soma and extended to one of the ends of that particular dendritic tree (see Fig. 6). The RAs from the unlesioned hemispheres were scanned for well-stained, isolated paths of dendrite that were, for the most part, parallel to the plane of focus. All brains were scanned, and of these 10 were found to have at least 2 such paths. After spine counts were done the brains were decoded, and it was found that 6 brains containing 16 paths had been counted for testosterone-treated females and 4 brains containing 15 paths had been counted for untreated females.

The counts were performed by aligning an eyepiece grid over the image of the dendrite in the microscope and counting individual spines within each box of the grid. At the magnification used, the side of a box on the grid corresponded to 8 μm. As the dendrite curved, the grid was rotated so as to keep it aligned with the orientation of the dendrite. The counts were segregated according to branching order. When a branch point was encountered, the proportion of the last box containing "pre-branch" dendrite was estimated as a fraction of 8 μm and a notation was made that the last spine count was of x/8th of a box. The grid was then repositioned to have a box start at the origin of the "post-branch" dendrite, on which the counts were to be continued. The graphs of spine density/8 μm bin in Figure 6 use these uncorrected bin counts. To generate corrected measures of the density of spines per micron, the number of spines per branch segment and per total path were divided by branch segment and total pathlength, respectively. The branch segment length and total pathlength were determined using the 3-dimensional computer-interfaced reconstruction system described in the following section. Spine counts yielded mean values of the number of spines/1 μm dendrite per cell and per bird. Comparisons between groups involved comparing the mean and median values of each group.

These computer-generated measurements of the length of dendrite paths used for spine counts were also directly compared for the T-treated and untreated groups. Since these were chosen without knowledge of the identity of the brain, they were taken to be samples of the length of the entire dendritic tree and should therefore have reflected the changes in length induced by testosterone treatment.

Electron microscopy. All thin-sectioning for electron microscopy was done with a diamond knife using a Reichart Ultracut ultramicrotome. Viewing and photography of thin sections were done on a Joel 100CX EM. Thin sections of Golgi-stained material to be kept for serial reconstruction of identified cells were mounted on Formvar-coated slot grids. Thin sections not taken for serial reconstruction were picked up with 400-mesh hexagonal copper grids. Sections were stained with uranyl acetate and lead citrate.

In order to reconstruct the dendrites of an identified neuron and map the occurrence of degenerating synapses on those dendrites, it was nec-

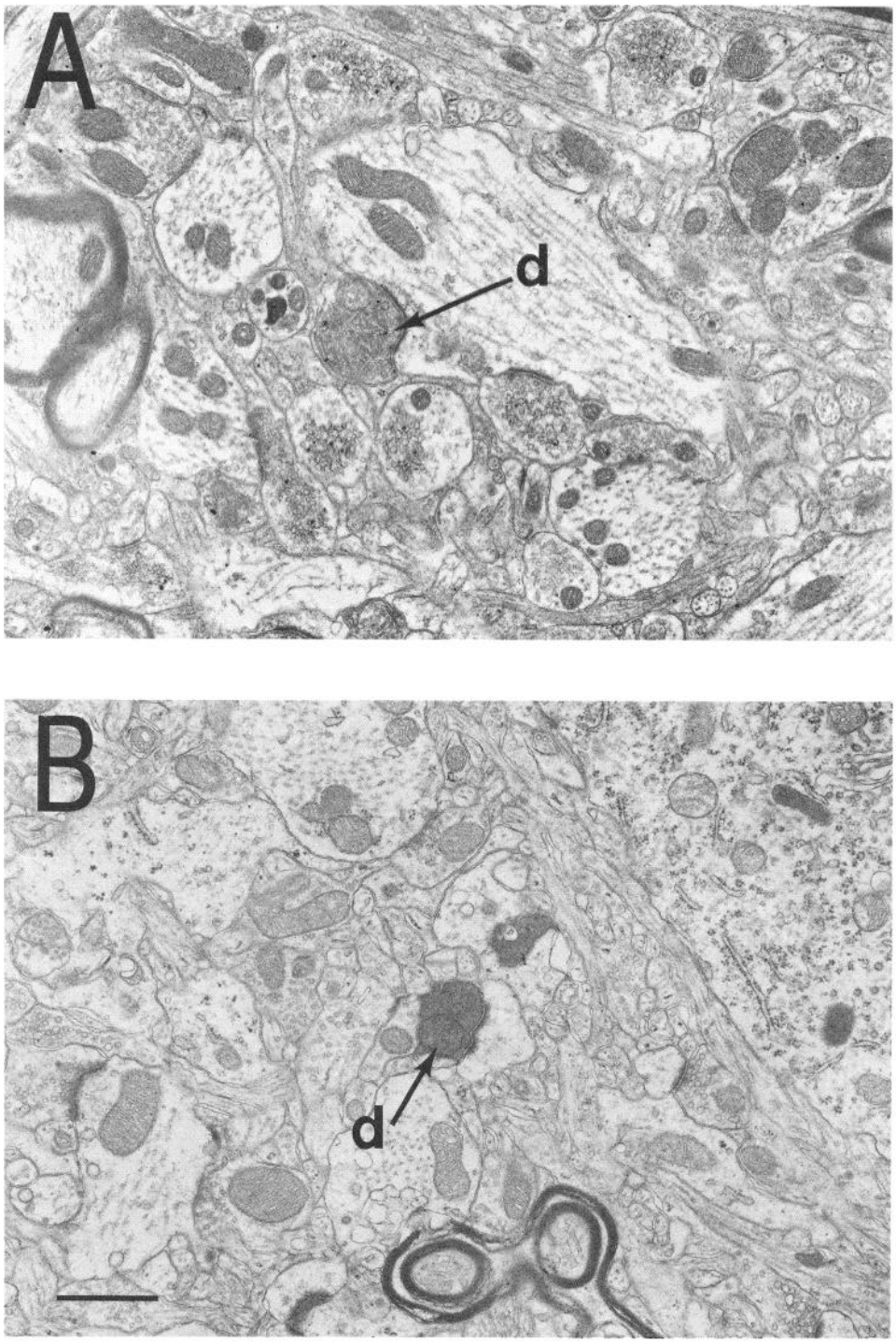

Figure 3. Effect of testosterone on the darkness of degenerating synapses. *A*, Testosterone-treated female. Degenerating synapse (*d*) is the result of a lesion to L-MAN made 107 hr before killing. Synaptic vesicles and presynaptic density can be seen. *B*, Normal female. Degenerating synapse (*d*) resulting from lesion of L-MAN made 72 hr before killing. The degeneration is much darker than that in *A*. (From Golgi-stained material.) Bar, 1 μm.

essary to first select and identify a neuron at the light-microscopic level in Golgi-stained 140-μm-thick plastic sections and then remount and resection that identified cell on an ultramicrotome for electron-microscopic analysis. Determining one's precise location on the identified cell when looking at a particular thin section (of which there can be as many as 1600 for a single cell) is at times a very difficult and time-consuming problem. The transition from the light-microscopic level, where the neuron in its entirety can be seen, to the electron-microscopic level, where individual synaptic profiles can be distinguished, was made through reference to (1) computer drawings of the identified cell's dendritic tree, recorded before it was cut for electron microscopy, (2) light micrographs of the cell taken at intervals during the cutting for electron microscopy, and (3) comparisons of various magnifications of the cell's dendrites as seen in thin sections, as well as careful documentation of stretches of dendrite as they were examined (Figs. 4, 5).

The computer drawings were obtained from digitized files of the identified Golgi-stained cells recorded through use of a computer-interfaced microscopy system (Wann et al., 1973; DeVoogd and Nottebohm, 1981a; DeVoogd et al., 1981). The files generated by this system contain a set of labeled coordinates that can be used to redraw a neuron's entire dendritic arbor and to determine the length of that arbor as well as the individual length of any portion of the arbor. Distances along the dendrite and between any 2 points entered can also be determined. The positions of synapses encountered at the electron-microscopic level were

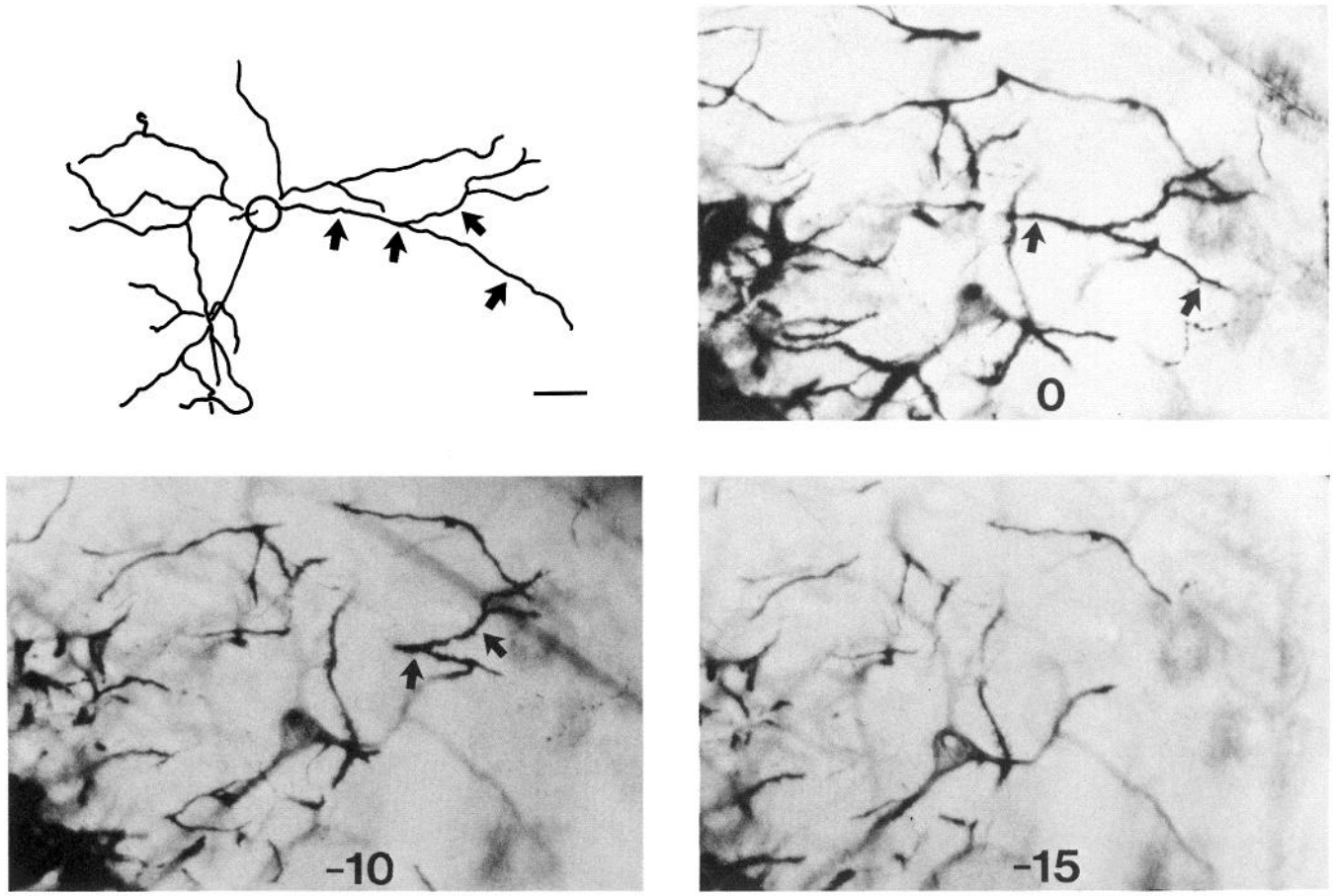

Figure 4. Sequential light micrographs of tissue as it is being cut for electron microscopy. *Upper left,* The computer-generated stick figure of a cell on which synapses degenerating as a result of a lesion to L-MAN were mapped. Bar, 20 μm. The 3 photographs are of the face of the block containing this cell as it was serially sectioned for electron microscopy. The cell body of a nearby cell and dendrites from other nearby cells are also seen. *Arrows* on the stick figure in the upper left panel indicate corresponding sections of dendrite in the *upper right* photograph that are missing in the *bottom left* photograph. *Bottom left,* The same block face after 10 μm of tissue had been cut into serial thin sections. *Bottom right,* The same block face after 5 more microns worth of thin sections had been taken.

recorded both in shorthand notation in a log book and by marking the appropriate position on the computer drawings generated from these files.

Light micrographs of the cell were made before sectioning had begun and every 60–70 thin sections thereafter (about every 5 μm) (Fig. 4). To take the latter photos, the chuck holding the Golgi-stained cells was pulled out of the ultramicrotome and light transmitted up through the block on which the tissue was glued so that a light photograph could be taken. These light photographs recorded the progress through the tissue, and in particular identified the position of a section of dendrite within the 1400–1600 thin sections taken for each cell. They also provided a view of the entire block face, including features such as blood vessels, cells not being studied, and the shape of the block face, which could then be related to structures seen at the electron-microscopic level. After taking a photograph, the chuck was repositioned as before so as to continue taking ultrathin sections without interruption.

Progress was recorded by shading those lengths of dendrite already examined on the computer drawing. By doing this, it was possible to keep track of which portions of a dendritic tree remained to be followed. This was very important because of the constant variation in the electron-microscopic cross-sectional shape of a given dendrite as it twisted and turned through space and as its relation to other landmarks changed. It was necessary to make a mental note of the relationship of a given profile with neighboring blood vessels, cell bodies, or other processes in order to be sure that the same process was being followed from its origin to its tip. There was always the possibility of confusion with the Golgi-filled dendrites from nearby cells. For this reason, only 3 or 4 segments of dendrite at a time were followed through successive thin sections. This meant that, as a dendrite branched, a decision had to be made as to which of the 2 new segments was to be followed. A notation was made on the computer figure of the cell to return at a later time to the segment that had not been followed.

Synapse identification. Of the Golgi/electron microscopy-processed animals, one from each of the 4 comparison groups (HVc or L-MAN lesion in either testosterone-treated or untreated females) was chosen for dendrite mapping of degenerating synapses. RA is a relatively small area, and when using the rapid Golgi stain, well-impregnated neurons within it occur unpredictably. Also, the lesions did occasionally leave some cells in the targeted nucleus undamaged (these animals were not used). It was therefore necessary to process a large number of animals in order to be sure of obtaining sufficient Golgi/electron-microscopic material.

Two morphological features were used to identify a degenerating profile as a synapse: the synaptic cleft and the postsynaptic density. In this material the synaptic cleft is a characteristic spacing between pre- and postsynaptic membranes of approximately 0.02 μm, and the postsynaptic density is a fibrous mat of electron-dense material found on the cell side of the postsynaptic membrane. In some cases in the Golgi-stained material, the postsynaptic density was difficult to distinguish because of the gold deposits of the Golgi stain. In these cases, if the synaptic cleft did not unambiguously define a synaptic zone, the degenerating profile was judged not to be a synapse.

Sampling for concentration of synaptic profiles. We were interested in estimating the number of synapses per unit volume of RA tissue. For this we used the same procedure with animals that had or had not received a lesion, regardless of whether the synapses counted were intact or degenerating ones. The tissue sampled came from the approximate center of RA. Electron micrographs were made at microscope magni-

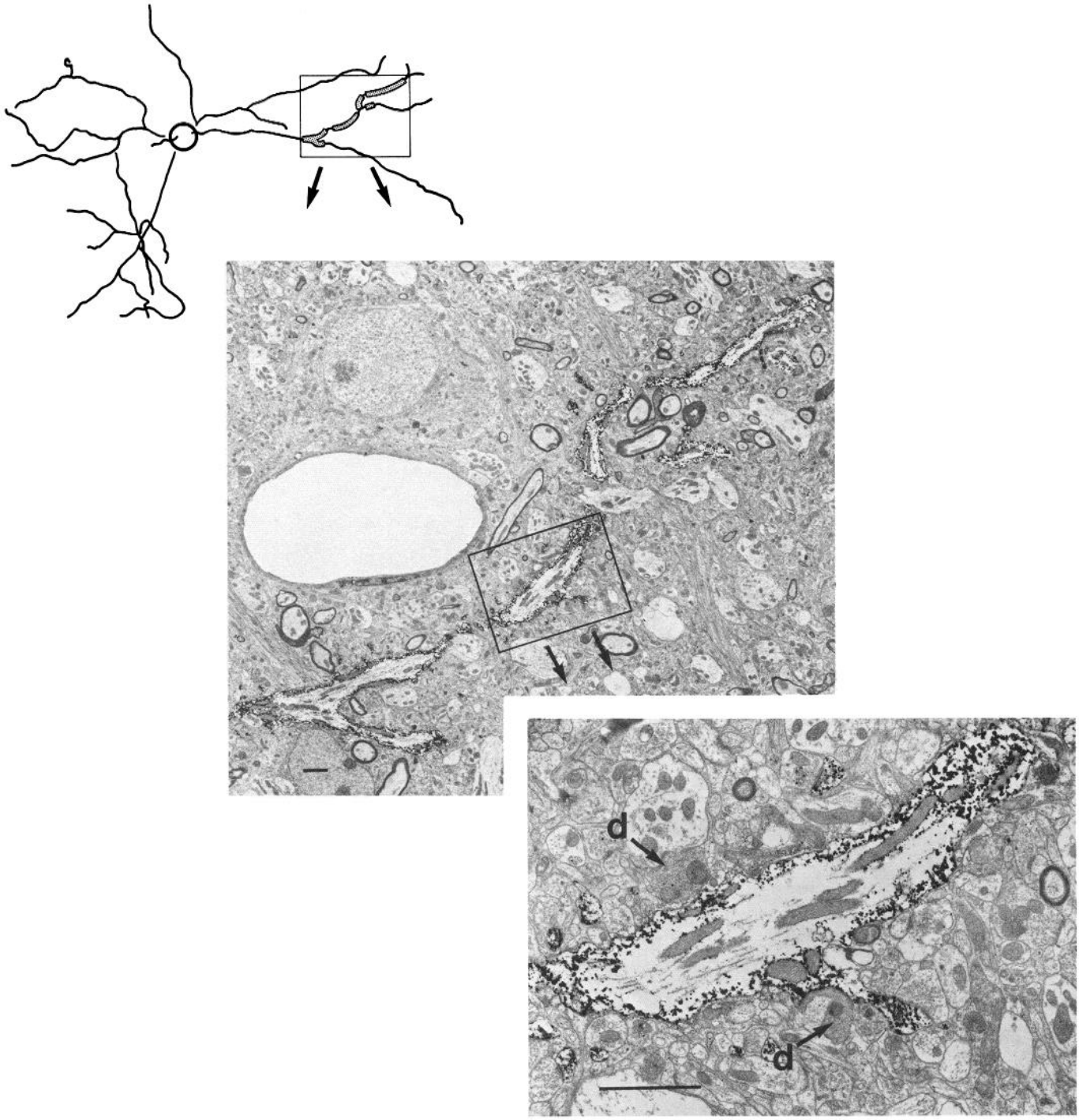

Figure 5. Computer-generated stick figure and EM photograph showing dendrite transected. *Inset, upper left,* Stick figure of same cell as in Figure 4, with EM photographs showing one transection of the gold-toned Golgi-stained dendrite of that cell. The *box* superimposed on the stick figure indicates the position of the lower-magnification EM photograph and the sections of dendrite that have been transected in the EM photograph are shown in *bold* on the stick figure. The higher-magnification photograph on the *lower right* shows 2 degenerating synapses (*d*), with the one on the *lower right* occurring on the Golgi-stained RA type IV cell. This degenerating shaft synapse actually occurs on the base of a small branchlet that was not recorded in the computer file for this cell. Bars, 2 μm.

fications of 5000 and 6600×. An effort was made at this stage to photograph only neuropil, and to avoid filling the frame with blood vessels, axon bundles, and cell bodies. The person taking the photographs was blind to the identity of the sections being sampled. For L-MAN-lesioned material, at least 5000 μm^2 of tissue was photographed. For HVc-lesioned material, at least 2000 μm^2 of tissue was sampled. (There were many more degenerating synapses following HVc lesions, so accurate estimates of concentration could be derived from smaller areal samples.) Synapses were then counted on prints at 12,500 and 16,000× (2.5× negatives) for each sample. For this material, too, a synapse was defined by its synaptic cleft and postsynaptic density; when they were observed, synaptic vesicles and presynaptic densities aided in identification.

The number of synapses per unit volume was estimated from the synapses per unit area obtained for each RA sampled using a formula derived by DeHoff and Rhines (1961, 1968). The derivation of this

formula assumes that a plane of infinite thinness will intersect particles with recognizable flat, circular ends with a frequency that is dependent on the size of the flat, circular ends and the number of particles within a unit volume of the sample. The section thickness used to sample for synapses in this study was approximately 0.08 μm, about one-third in diameter of the smallest synaptic profile detected in this sample, one-twentieth the size of the largest and one-sixth the size of the overall average synapse diameter. Obviously, in this case, 0.08 μm is not infinitely thin with respect to the size of the particle being counted. Therefore, the number of synapses encountered by the thin sections is higher than what would be obtained with an infinitely thin section, and the estimate of the number of synapses per unit volume is somewhat higher than it should be.

The formula from DeHoff and Rhines (1961) used to estimate synapses per unit volume (S_V) from synapses per unit area (S_A), as measured in the EM photographs, is

$$S_V = (8 \times S_A \times z)/n \times \pi,$$

where z is the average of inverse profile lengths of the synapses counted, as measured from photographs with a data tablet, and n is a weighing factor based on the number of flat, circular ends of the particle whose density is being estimated. The value of n would be 2 if what was being measured was a cylinder with 2 flat ends. Since what is being measured is a sphere with one flat end (a synaptic bouton with a synapse at one end), however, n should be 1. The value of 1 assigned to n assumes a recognition of discontinuities occurring in synaptic appositions. There is the possibility that synapses with perforated synaptic zones were counted as 2 separate synapses if the discontinuity caused by the perforation was not recognized. The occurrence of perforated synaptic zones was estimated by DeVoogd et al. (1985) to be 10–15% in the central RA of female canaries. This estimate was not found to differ between normal and testosterone-treated females in that study. Thus, assigning n a value of 1 could result in an overestimation of the number of synapses, but this overestimation should not differ for RAs of normal and testosterone-treated female canaries.

Results

Overall synaptic density in RA

RA volume. The mean R + L RA volume was 0.136 mm³ (SD = 0.044) for the untreated females ($n = 8$) and 0.255 mm³ (SD = 0.044) for the testosterone-treated females ($n = 9$). This difference is significant ($t = 5.57$: $df = 15$; $p < 0.001$; 2-tailed test). The 87% increase in RA volume is similar to that reported in a previous EM study (DeVoogd et al., 1985) and is slightly larger than that reported in a previous Nissl study of intact 2-year-old females (Nottebohm, 1980).

Changes in the total number of L-MAN and IIVc synapses in female canary RA with testosterone treatment. The concentration per unit volume of all synapses, considered together, was less in testosterone-treated (0.863/μm³; $n = 5$ animals) than in normal female (1.23/μm³; $n = 4$ animals; $p < 0.01$; 1-tailed) RAs. This decrease in concentration is in agreement with previous work (DeVoogd et al., 1985). However, since the average total volume of RA increased by 87% in the testosterone-treated females, the estimate of the total number of synapses per RA is actually 28% higher in the testosterone-treated females than in the untreated females. This estimate of the increase in total synapse numbers in RA following testosterone treatment is lower than that reported by DeVoogd et al. (1985), which may be due to differences in the estimation methods used (Canady, 1986).

The concentration of degenerating synapses per unit volume resulting from HVc lesions was 0.176/μm³ ($n = 5$; median, 0.137; range, 0.103–0.304) in untreated females and 0.234/μm³ ($n = 3$; median, 0.184; range, 0.183–0.336) in testosterone-treated females (NS). Relating these concentration values to the average difference in total RA volume between untreated and testosterone-treated adult canaries shows that the average total number of these synapses in RA actually increases 2.4-fold (1.2×10^7 for untreated females and 2.9×10^7 for testosterone-treated females).

The concentration of degenerating synapses in RA resulting from L-MAN lesions also did not differ significantly between normal and testosterone-treated females, though in this case, too, the estimated total number of such synapses in RA was higher in testosterone-treated females. The mean concentration values were 3.3×10^{-3}/μm³ ($n = 4$; median, 3.1×10^{-3}; range, 2.1×10^{-3}–5.0×10^{-3}) and 6.5×10^{-3}/μm³ ($n = 4$; median, 6.1×10^{-3}; range, 2.1×10^{-3}–1.0×10^{-2}), which gave estimates of the total number of L-MAN synapses in RA of 2.2×10^5 and 8.1×10^5 for untreated and testosterone-treated females, respectively. This is a 3.7-fold increase in the total number of synapses from L-MAN in RA as a result of testosterone treatment. (If there were no difference in the number of HVc and L-MAN synapses per unit of RA volume between the testosterone-treated and untreated females then synapses from both sources would have increased by just a factor of 1.87—the difference in RA volumes between treated and untreated females.)

Further comparisons of the concentrations of intact and degenerating profiles suggest that much of the testosterone-induced synaptogenesis in RA can be accounted for by the increases in these 2 sources, and that HVc in particular could account for 76% of the increase in all synapses in RA with testosterone treatment. The average overall increase in the number of synapses in RA with testosterone treatment is 2.3×10^7 (10.7×10^7 for testosterone-treated females minus 8.4×10^7 for untreated female RAs). The increase due to testosterone treatment in synapses resulting from HVc lesions is 1.7×10^7 and from L-MAN is 5.9×10^5. The sum of these is 1.759×10^7, which, divided by 2.3×10^7, is 0.76.

General findings on type IV cells

Dendritic length following testosterone treatment. The average length of type IV cell dendrites that coursed parallel to the plane of section, from their origin at the soma to their tip, was 115.7 μm in the untreated females (15 dendrites obtained from 4 brains, as described under Materials and Methods) and 133.3 μm in the testosterone-treated females (16 dendrites obtained from 6 brains). This increase of 15% is significant ($t = 3.26$; $df = 8$; $p < 0.02$; 2-tailed test). The magnitude of this difference is probably an underestimate, since the condition set for accepting a dendrite—that it travel parallel to the plane of section—would tend to penalize the longer dendrites, which would be more likely to meander away from the plane of section. Also, the measure of length of one dendrite from origin to tip is not directly comparable to the measures of total dendritic length for a whole dendritic tree made in previous studies. Despite these reservations, the results obtained are surprisingly similar to those of DeVoogd and Nottebohm (1981b), in which the overall dendritic length of type IV cells in females that had been ovariectomized as juveniles and treated with testosterone at 1 year of age was 22% greater than that of intact females of the same age. Because of this similarity in results, we will use the estimate of overall dendritic length per type IV cell reported by DeVoogd and Nottebohm (1981b) as a conservative estimate of the consequences of giving testosterone to intact female canaries.

Number of spines on type IV cells. There are 3 sources of error that should be considered concerning the way the spine counts were done. The first is that the spines were at times difficult to

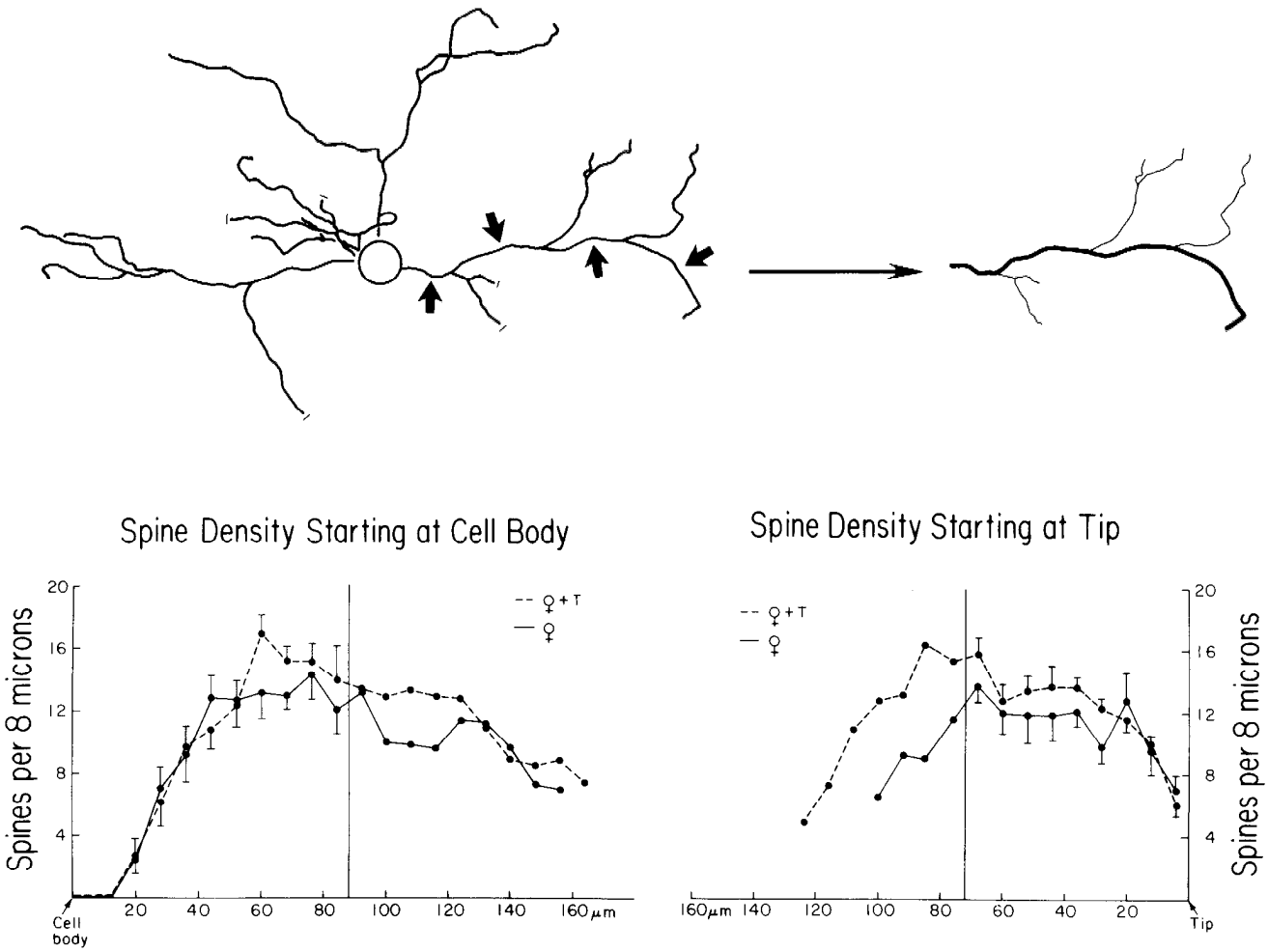

Figure 6. Spine density on dendrites of type IV neurons compared between normal and testosterone-treated female canaries. *Top,* On this computer-generated stick figure of a type IV neuron, *short arrows* point to an example of a "path" of dendrite extending from the cell body to one dendrite end of a particular tree. This path of dendrite on which spines were counted is shown in *bold* to the right. *Lower left,* Number of spines/8 μm bin as a function of 2-dimensional distance from the dendrite origin, where the "paths" are now lined up at their origins. The shorter "paths" begin to end at their tips as one moves to the *right. Lower right,* Number of spines/8 μm bin as a function of two-dimensional distance from the tips of the dendrites. Now the shorter paths begin to end at their origins as one moves from right to left. The *vertical solid line* in the 2 parts on the bottom indicates the point where the densities of individual "paths" begin to reach 0. Values beyond this line are, for this reason, unreliable.

distinguish. When spine density was high, clumps of spines occurred in ways that may have obscured individual spine heads and necks. The second source of error is that the dendrite trunk obscured a number of spines that occurred below it, whose spine necks were too short to be seen clearly through or around it. A third source of error is due to the curving, snakelike path that the dendrite takes through the field of view. Changes in direction perpendicular to the plane of focus influenced the number of spines seen in a particular grid box, and these changes in direction could not be corrected for. This was the reason for taking great care in selecting paths of dendrite that ran parallel to the plane of focus.

Figure 6 shows the number of spines counted per successive 8 μm grid box as one moves out from the soma to the tip of the dendrite (lower left), and as one moves from the tip of the dendrite to the soma (lower right). The graphs in Figure 6 represent the same data and are animal means, with several cells sampled for each animal (see below). In the lower left of Figure 6 we see that the first 20–30 μm of dendrite is relatively free of spines, and that the spine concentration rises quickly for both the untreated and testosterone-treated groups. In the lower right of Figure 6, we see that the concentration falls near the tips of the dendrites in both the testosterone-treated and untreated groups.

If one subtracts the first 30 μm from the average 4.6 and 4.1 first-order dendrites occurring, respectively, in the type IV cells of testosterone-treated and untreated females, then there is an average of 2090 and 1679 μm spine-bearing dendrites, respectively, per type IV cell of those 2 groups (DeVoogd and Nottebohm, 1981b). Using total number of spines counted, divided by the actual 3-dimensional length of the dendrites, the average spine density for third-order dendrite segments (segments beginning 2 branch points away from the cell body) is 1.38 countable spines/μm for the untreated female canaries (animal means using 15 dendrites in 4 animals; median of animal values, 1.42), which yields an estimated number of spines per type IV cell of $1679 \times 1.38 = 2317$. The testosterone-treated females had 1.63 countable spines/μm of third-order dendrite (16 dendrites in 6 animals; median, 1.66), yielding an estimated $2090 \times 1.63 = 3407$ spines per type IV cell. These estimates suggest that testosterone treatment of female canaries results in an average increase of 1090 new spines per RA type IV cell. Were each

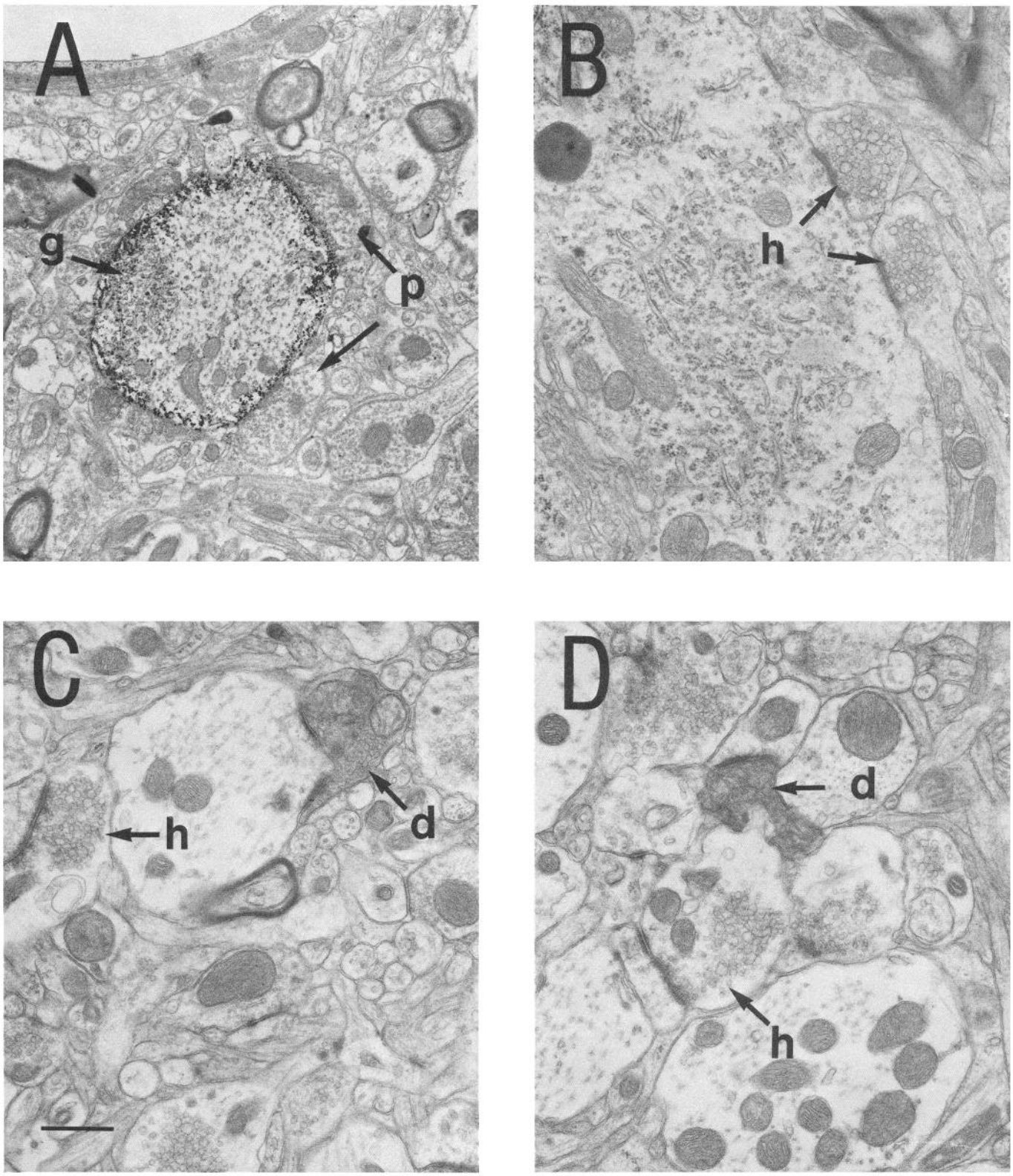

Figure 7. Normal and degenerating synapses in RA. *A,* Golgi-filled process (*g*) is dendrite close to the cell body of a type IV cell. Two synapses (*p*) that occur at this proximal location have symmetric pre- and postsynaptic densities and small synaptic vesicles. *B,* Two somatic synapses (*h*) on an unidentified neuron in RA. Since somatic synapses do not occur on type IV cells, it is at least known that this is not a type IV cell. These synapses are of the type that is not present in the RAs of HVc lesioned animals, and so are thought to be HVc synapses. *C,* HVc synapse (*h*) occurring on a spinous process and one synapse in an early stage of degeneration (*d*) resulting from lesion of L-MAN, occurring on a dendrite shaft. *D,* One degenerating L-MAN synapse (*d*) occurring on small process that is likely to be a dendrite shaft, and one HVc synapse (*h*) occurring on a spine. Bar, 1 μm.

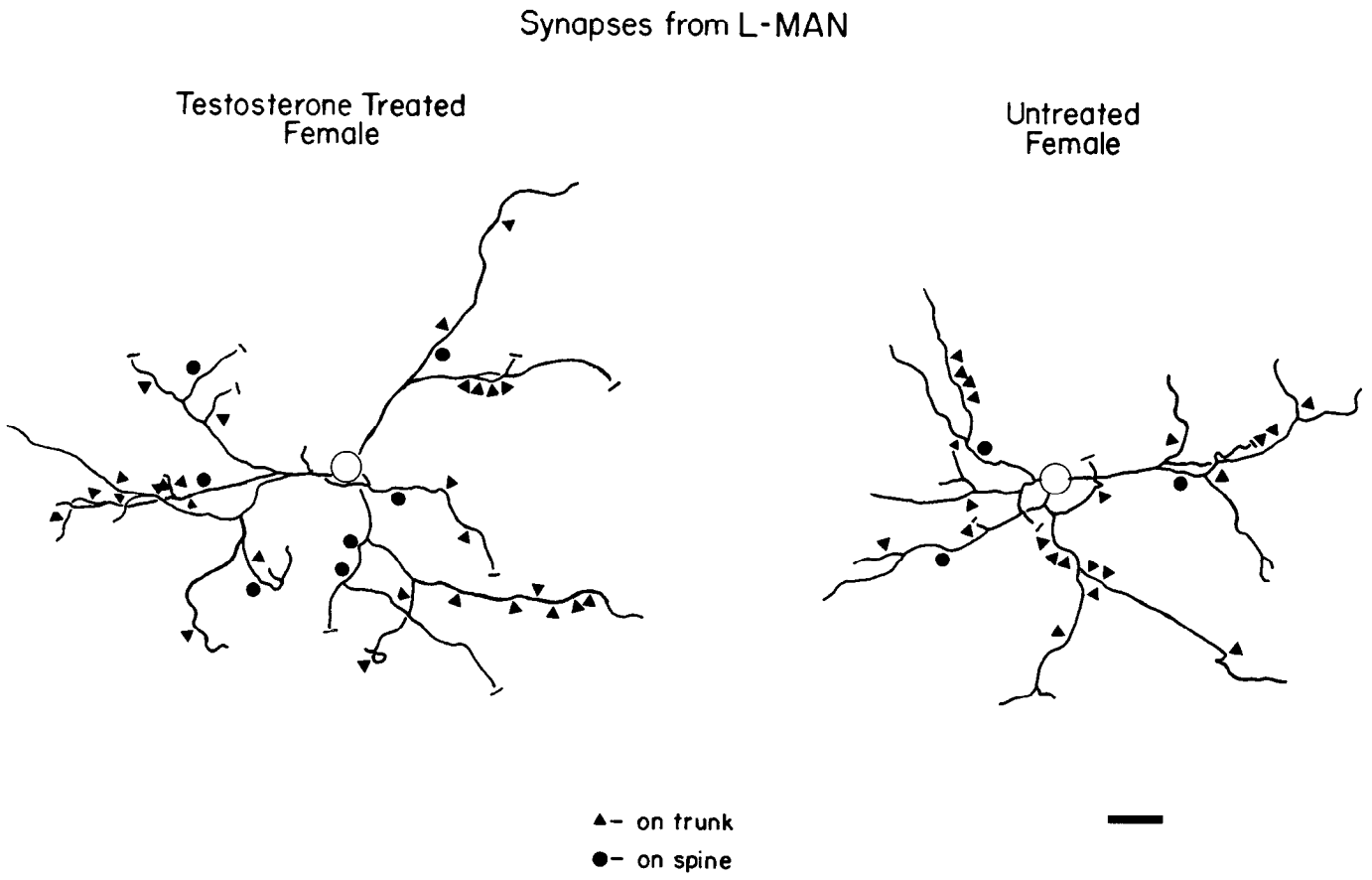

Figure 8. Locations of degenerating synapses on type IV neurons resulting from lesions of L-MAN. Computer-generated stick figures of representative type IV cells for testosterone-treated and normal female canaries. The dashes (–) at the ends of some of the segments indicate that the dendrite had left the section, and so could not be mapped further. Bar, 20 μm.

spine to receive one synapse, then the type IV cells of the testosterone-treated birds would receive a 47% increase in the number of synapses formed on spines.

Comments on the electron-microscopic morphology of type IV cells. A complete examination of the location and morphology of the various synapse types formed on RA type IV neurons has not been completed, but we have made the following observations. First, no synapses were encountered on the somata of type IV neurons. The closest synapses do not appear until at least 10 μm away from the soma. We encountered other cells in RA that did have many synapses on both the soma and proximal dendrite (Fig. 7*B*). However, these cells were not identified, and it is not known which neuron class they belong to. The most proximal synapses that were encountered on identified type IV neurons contained flattened vesicles and had symmetric pre- and postsynaptic densities (Fig. 7*A*). This morphology, along with the location, suggests that these synapses are inhibitory (for example, see Matus and Dennison, 1971; Gottlieb and Cowan, 1972), and that they exert a major influence on the excitation of the cell when they are active. Synapses of a similar morphology were found occasionally on the necks of dendritic spines on type IV cells. Again this suggests an inhibitory role for this type of synapse (Kemp and Powell, 1971; Wilson et al., 1983). In the latter case, the inhibition is of a highly selective nature, acting more directly on specific inputs to a cell rather than influencing an entire dendritic tree. Since these synapses were never encountered in a degenerate state, they are not likely to be of HVc or L-MAN origin; therefore, the inhibition they might convey is likely to come from neurons within RA.

Endings from identified sources on type IV neurons

Lesions of both L-MAN and HVc resulted in degenerating synapses on type IV neurons. The absolute number and the type of degenerating synapses differed markedly depending on whether HVc or L-MAN had been lesioned. Unfortunately, we do not have enough independent samples for a meaningful comparison of the number of synapses of known origin received by type IV cells in treated and untreated females.

L-MAN synapses. Six neurons were mapped for degenerating synapses from L-MAN. Of these, 3 came from an untreated female and 3 came from a testosterone-treated female. The synapses fell on both spines and trunks of the dendrites. For each L-MAN synapse ending on a spine, 2.5 L-MAN synapses ended on trunks. These degenerating synapses were distributed all along the dendrite, starting approximately 30 μm out from the soma (Fig. 8 shows 2 examples, one from a testosterone-treated female and one from an untreated female). The total number of degenerating synapses counted on the 6 cells sampled was divided by the total length of dendrite mapped on those cells. This was multiplied by the average length of dendrite for untreated and testosterone-treated females (DeVoogd and Nottebohm, 1981a, b) in order to estimate the number of synapses an average type IV neuron might receive from L-MAN. The estimate obtained in this manner is approximately 50 L-MAN synapses/type IV

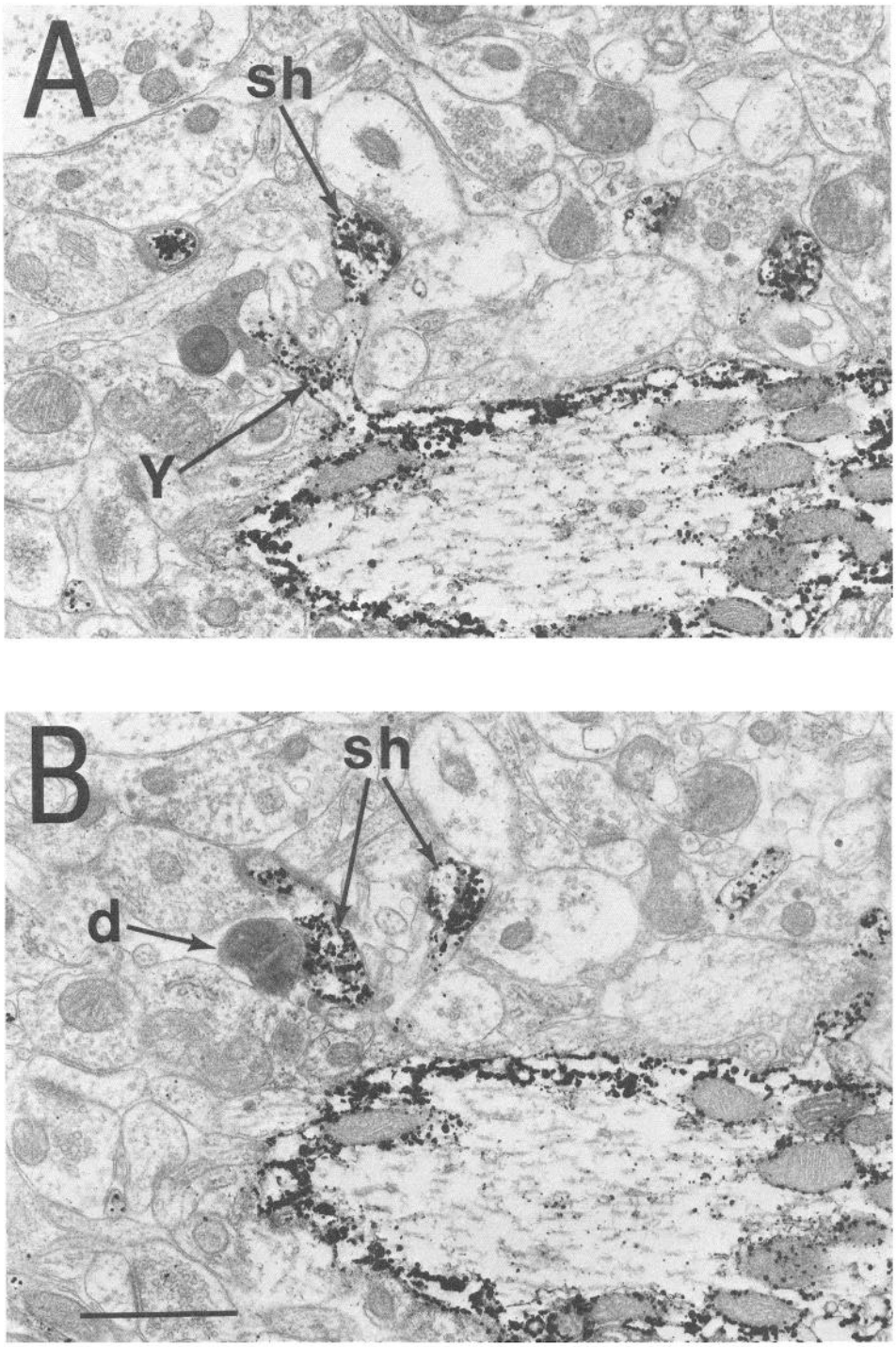

Figure 9. Y-shaped spine. *A, B,* Two thin sections containing portions of the same Golgi-stained, identified type IV neuron. The Y-shaped structure in *A* is a spine neck giving rise to 2 spine heads (*sh*), each bearing a synapse. In *B,* the *left-hand branch* of the Y can be seen to synapse with a degenerating bouton (*d*), which identifies it as an L-MAN synapse. L-MAN lesion in a testosterone-treated female, 108 hr survival after lesion. Bar, 1 μm.

cell, ignoring differences that might arise due to testosterone treatment.

Early stages of degeneration (at shorter survival times than those used for mapping), when the synapses from L-MAN are already darker than other synapses but cytological details can still be discerned, show that synapses from L-MAN have asymmetric pre- and postsynaptic densities and contain vesicles of a medium diameter relative to those in other synaptic boutons in RA (see Figs. 3*A*, 7*C*). The average length of the synaptic apposition of L-MAN endings in RA encountered in both the untreated and testoterone-treated samples, as morphologically defined by the synaptic cleft, was 0.58 μm. Since the average length of all chords through a circle is $\pi/4$ times the diameter of that circle, this average profile length places the average synaptic apposition disk diameter at approximately 0.74 μm, assuming a flat disk (see Hilman and Chen 1985). There are synapses with similar features, also on type IV cells, that do not degenerate when L-MAN is lesioned and which, therefore, are presumably not from L-MAN.

One very intriguing aspect of the L-MAN synapses on type IV cell spines is that they appear to occur predominantly, if not exclusively, on Y-shaped or branched spines having a single

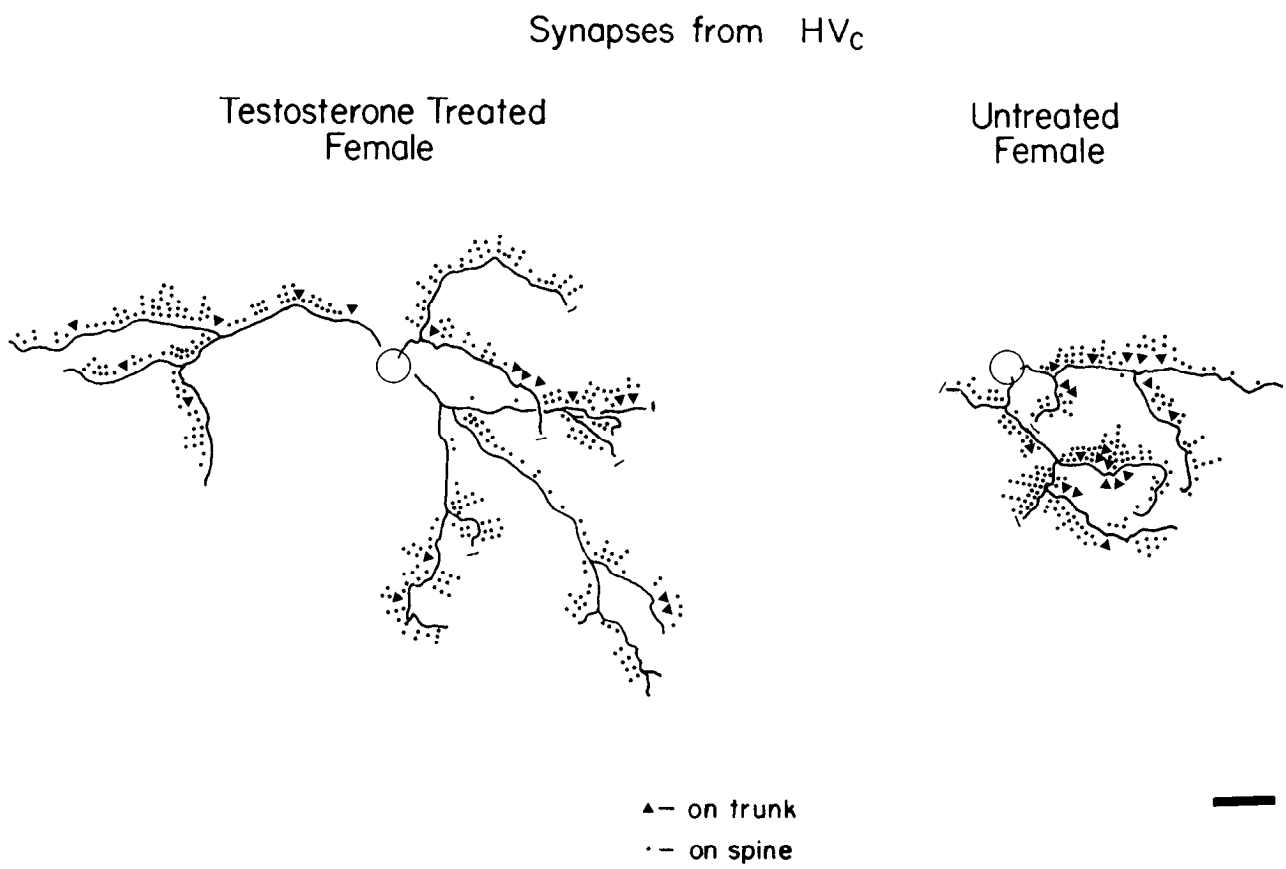

Figure 10. Locations of degenerating synapses on type IV neurons resulting from lesions of HVc. For easier comprehension, one dendrite for the testosterone-treated female type IV neuron and unmapped dendrites of the untreated female type IV cell were not drawn here. The dashes (–) at the ends of some of the segments indicate that the dendrite had left the section and so could not be mapped further. Bar, 20 μm.

stalk attached to the dendritic shaft and bearing 2 spine heads (Fig. 9). In 5 cases of degenerating L-MAN synapses contacting spines that were examined closely in serial reconstructions, all had been part of these dyads that included the degenerating L-MAN synapse and a nondegenerating synapse. It is not clear at this time whether these Y-shaped spines represent a novel arrangement of synaptic confluence or a regenerative state due to the removal of the L-MAN input. Interestingly, Y-shaped spines have also been observed at the light-microscopic level on RA type IV cells in animals that had not had lesions in either L-MAN or HVc. At the light-microscopic level, Y-shaped spines on type IV cells are most easily seen in untreated females, where the lower density of spines allows a clearer view of individual spines, but they have also been observed in testosterone-treated females and in males. Structures like these have been observed in other systems (Carlin and Seikevitz, 1983; Wilson et al., 1983; Shieh et al., 1984; see also Fig. 5 of Matsumoto and Arai, 1979).

HVc synapses. Following HVc lesion, 19 of every 20 degenerating synapses observed on type IV cells are on spines. The twentieth degenerating synapse is seen on the shaft. As we saw in the previous section, the majority of L-MAN inputs to type IV cells are on dendritic shafts. Since it is very difficult not to interfere with the axons that travel from L-MAN to RA when lesioning HVc, the shaft synapses observed may in fact be L-MAN synapses (see Materials and Methods). If one now takes the number of HVc synapses formed per micrometer of dentritic length of type IV cells and divides this number by the number of spines per micrometer of dendritic length of the same cell type, we see that approximately one out of every 3 spines of type IV cells receives input from HVc.

The degenerating synapses on type IV cells resulting from lesion of HVc were much more numerous than those from lesion of L-MAN (Fig. 10). A type IV cell may receive on the order of 1000 HVc contacts (derived as above with total L-MAN synapses). It would seem, then, that the ratio of HVc to L-MAN inputs to type IV cells is 20:1. This ratio strengthens our suspicion that the 1 in 20 synapses that, after HVc lesion, degenerates on a type IV cell dendritic shaft is of L-MAN origin. Therefore, it seems likely that *all* of the HVc inputs on type IV cells are on spines.

The profiles of synapses from HVc were smaller than those from L-MAN. The average diameter of the synaptic apposition disk is 0.46 μm for HVc synapses formed in RA (vs 0.74 for synapses from L-MAN). Since the HVc synapses were so numerous, it was possible to compare RA tissue from HVc-lesioned and intact females to see what a nondegenerating HVc synapse looks like simply by observing which synapse type disappeared after lesion. (This assumed that only one synapse type found in RA originated from HVc.) One synapse type observed to be present in RA in canaries with intact HVcs, but missing in RA in canaries whose HVcs had been lesioned, had asymmetric pre- and postsynaptic densities, and had large polymorphic vesicles away from the synaptic zone with medium-sized vesicles lined up at the synaptic apposition (Fig. 7, *B–D*). These asymmetric synapses with large polymorphic vesicles formed not only on type IV dendrites, but also on the somas of at least

one another cell type (Fig. 7*B*). Thus, if such synapses come exclusively from HVc, then HVc input to RA is not restricted to type IV neurons.

Qualitative appraisal of the number of HVc and L-MAN synapses on the dendritic ends of type IV neurons in normal and testosterone-treated females

An earlier study showed that when adult female canaries are treated with testosterone, the length of the more proximal segments of dendrite remains unaltered, but that the number and length of end branches increases (DeVoogd and Nottebohm, 1981b). That is, new dendritic length seems to appear in the form of new or longer terminal branches. We were particularly interested in finding out what kind of inputs are received by these newly grown dendritic segments. Specifically, since both HVc and L-MAN are testosterone-sensitive, it was anticipated that one or both of these inputs might be added to the new dendrite in preference to other sources of synaptic input. In other words, the transition from normal female vocalizations to testosterone-induced male-typical songs might involve a selective addition of either L-MAN or HVc inputs to type IV cells. If this selective change in synapse concentration is occurring at the growing ends, there should be a dramatic shift in the concentration of HVc or L-MAN inputs there. Conversely if another spinous input is selectively added (from intrinsic or unknown extrinsic sourses), then there might be an equally obvious lack of HVc synapses, since these synapses occur frequently all along the dendrite in untreated females. To see whether, within these constraints, a clear selection of synapses was occurring on the newly grown dendrite, a serial electron-microscopic survey was made of the dendrites of type IV cells in HVc and L-MAN lesioned untreated and testosterone-treated female canaries. It was not our intention to discover small changes in the concentration of synapses at any point along the dendrites using these electron-microscopic reconstructions, but rather to determine whether a more general "strategy" for selective addition of synapses to testosterone-induced growing dendrites existed.

Females ovariectomized as juveniles and treated with testosterone in adulthood add an average of 396 μm of dendrite to their RA type IV cells (DeVoogd and Nottebohm, 1981b). The average number of ends for testosterone-treated female RA type IV cells is 24.45 (T. J. DeVoogd and F. Nottebohm, unpublished observations). If testosterone causes all dendritic ends to grow equivalently, then the last 396/24.45 = 16.2 μm of each dendritic end of the testosterone-treated females is "new" dendrite. This estimate is close to that obtained from comparing the length of dendrite paths parallel to the plane of section in untreated and testosterone-treated females (133.3 − 115.7 = 17.6 μm; see *General findings* in this section). Because of these considerations, dendritic reconstruction was used to determine the source of input received by the distal 20 μm of dendritic branches.

Six RA type IV cells were mapped for degenerating synapses resulting from complete ablation of L-MAN, 3 in an untreated female canary and 3 in a testosterone-treated female canary. These 6 cells have already been mentioned. Representative examples of these cells are shown in Figure 8. Particular attention was paid to finding and characterizing the ends of the dendrites on these 6 cells.

Seven RA type IV cells were sampled for concentration of degenerating synapses resulting from complete ablation of HVc, 3 in a testosterone-treated canary and 4 in an untreated canary. Because of the very high number of degenerating synapses per cell resulting from HVc lesions, attention was focused on the ends of the dendrites, where growth was thought to occur, at the expense of not having a sample of cells whose dendrites were completely mapped. One cell from an untreated female had virtually the entire length of one dendritic tree mapped, and one cell from a testosterone-treated female had virtually all of its dendritic length sampled. Three other cells from a testosterone-treated animal and 2 other cells from an untreated animal had only the distal 20 μm of one dendrite segment mapped. The 2 more completely mapped cells are shown in Figure 10.

Qualitative appraisal of the last 20 μm of each of the dendrites that were followed to their tips did not reveal a difference between the testosterone-treated and untreated cases in the number or distribution of degenerating synapses contacting the dendrites. In both the testosterone-treated and untreated cases, degenerating synapses were seen within the last 20 μm of dendrite; however, neither a dramatic increase nor a decrease in their numbers indicative of a discrete change in the circuitry was seen.

Discussion

Anatomical considerations

RA type IV cells are long projection neurons that connect RA to the hypoglossal motor neurons that innervate the muscles of the trachea and syrinx (R. A. Canady, D. Vicario, and F. Nottebohm, unpublished observations). Type IV cells are sexually dimorphic, with a larger dendritic tree in males than in females (DeVoogd and Nottebohm, 1981a). Levels of testosterone that induce adult female canaries to sing in a malelike manner also induce dendritic growth in their type IV cells (DeVoogd and Nottebohm, 1981b). We now know that type IV cells receive input from HVc and L-MAN. This is interesting because RA, HVc, and L-MAN have all been shown to be involved in the control of learned song (Nottebohm et al., 1976; Nottebohm et al., 1982; Bottjer et al., 1984).

HVc and L-MAN inputs to type IV cells differ in that, whereas the former end predominantly on spines, are smaller, and more numerous, the latter end more often on dendritic shafts than on spines, are larger, and less numerous. Otherwise, our data do not allow us to calculate what fraction of the inputs to type IV cells is contributed by HVc and L-MAN. However, we know that only one-third of the spines on type IV cells receive inputs from HVc and that an average of only about 14 of the remaining 2000 spines/type IV cell receive inputs from L-MAN. Thus, even if we restrict ourselves to the dendritic spines of type IV cells, about two-thirds of the synapses formed there remain unaccounted for and are presumably contributed from within RA. We do not know how many synapses form on the shafts of the type IV cells.

Type IV cells have some Y-shaped dendritic spines. Those that were analyzed ultrastructurally had one synapse on each arm of the Y, and in each of these cases, one of the synapses was from L-MAN. We do not know what the significance of this arrangement might be.

Four observations suggest that the overall number of synapses on type IV cells increases with testosterone: (1) the dendritic length of type IV cells increases; (2) the number of spines per unit of dendritic length in type IV cells remains the same or increases; (3) the total number of synapses in RA increases; and (4) type IV cells are probably the most common type of RA cell—at least they are the most common type in Golgi-stained material. It seems reasonable to conclude that a significant frac-

tion of the testosterone-induced increase in the number of synapses in RA occurs on type IV cells.

The distribution of HVC and L-MAN inputs on the dendritic tree of type IV cells seems not to be grossly affected by hormone. Type IV cells of both untreated and testosterone-treated females show (1) a similar distribution of dendritic spines at the light-microscopic level; (2) a similar distribution of L-MAN inputs along the entire dendritic tree; (3) a similar distribution of HVc inputs mapped from soma to dendritic tips; (4) a similar number of identified inputs in the distal 20 μm of dendrites. This is qualitative evidence. Many more data points are needed to make statistically valid quantitative statements.

A lack of qualitative differences in the distribution of L-MAN and HVc inputs on type IV cells of untreated and testosterone-treated females would be expected if the newly added dendritic length received a balance of inputs similar to that of preexisting dendrites. In the grossest sense, the hormone-induced increase in the number of inputs could then be characterized as "more of the same." Of course, we do not know whether, following testosterone treatment, a different (greater?) array of HVc and L-MAN cells now contacts each RA type IV cell. Nor do we know whether synapses that predated the onset of testosterone treatment remain in place. Possibly, the new inputs are distributed throughout the synapse-bearing regions of the entire dendritic tree, including the new, as well as the "old," dendrites.

We have so far discussed hormone-induced dendritic growth and synapse formation. Obviously, these effects must be mirrored by the axonal endings that provide the new synapses. Interestingly, not only RA, but also both HVc and L-MAN, contain androgen-concentrating subsets of cells (Arnold et al., 1976; Arnold, 1980). However, we do not know whether RA type IV cells fall into this category, nor do we know if the HVc and L-MAN cells that project to RA concentrate androgen in their nuclei.

It is too early to say how the microanatomical details discussed in the present report relate to song, if at all. However, this kind of circuit detail is needed to explain how song-control pathways function and how they are affected by hormones and experience. In addition, our observations may be applicable to other systems that are also modulated by hormones and learning.

Behavioral considerations

Nucleus RA is part of the motor pathway for song control in canaries, and its circuitry may be influenced by learning. RA also processes auditory information and may play a role in auditory perception (Williams and Nottebohm, 1985). The stereotypy of adult male canary song is associated with high plasma testosterone levels (Nottebohm et al., 1987) and with intact hearing (Nottebohm, et al., 1976). Likewise, the song of untreated female canaries is unstable and reminiscent of that of juvenile males (Pesch and Güttinger, 1985; F. Nottebohm, unpublished observations), but becomes relatively stereotyped after 3 or 4 weeks of testosterone treatment (Nottebohm, 1980; Pesch and Güttinger, 1985; DeVoogd, 1986). We do not yet know whether the hormone-induced transition from variable to stereotyped song in female canaries involves learning.

Testosterone-induced growth of RA in adult female canaries occurs whether such birds have intact hearing or are deaf, but the increase is greater in females with intact hearing (Bottjer et al., 1986). Thus, the testosterone-dependent results reported here may include both hormonal and experiential effects.

It has been suggested that the summer drop in adult male canary testosterone levels, which is associated with reductions in RA volume and song stereotypy, is a necessary condition for recurrent seasonal song learning (Nottebohm, 1981). Adult male canaries add many new song syllables during the summer and early fall, but few syllables are added thereafter, as testosterone levels rise and a large RA volume is restored (Nottebohm et al., 1986, 1987). By analogy, the high testosterone levels that induce RA growth and song stereotypy in adult female canaries might interfere with further song learning after RA growth and song stereotypy have been achieved. This possibility highlights the double effect that testosterone may have in the adult canary song-control system, namely (1) stereotyped mastery and retention of an acquired motor skill, and (2) inhibition of further song learning.

"Learning" and "conservation of learned information" may, to some extent, be 2 distinct and incompatible processes. Open-ended learners, such as the canary, are able to modify their song in adulthood and will forget it following deafening. Critical period learners, such as the white-crowned sparrow, learn their song once, before they reach sexual maturity (Marler, 1970), and retain it after deafening (Konishi, 1965). Fluctuations in the plasma testosterone levels of adult white-crowned sparrow males have no effect on RA volume (Baker et al., 1984), suggesting that there may be a relation between open-ended learning (and forgetting) and the anatomical responsiveness to testosterone shown by the adult canary song-control system. In the white-crowned sparrow, knowledge mastered seems to have permanently replaced the flexibility to learn, and perhaps even to forget.

The hormone-dependent changes we describe in the RA circuitry of adult canaries may eventually help us understand cell and circuit properties that allow some birds to learn new songs throughout their life, while others have this gift for only a few months.

References

Arnold, A. P. (1980) Quantitative analysis of sex differences in hormone accumulation in the zebra finch brain: Methodological and theoretical issues. J. Comp. Neurol. *189:* 421–436.

Arnold, A. P., F. Nottebohm, and D. W. Pfaff (1976) Hormone concentrating cells in vocal control and other areas of the brain of the zebra finch. J. Comp. Neurol. *165:* 478–512.

Baker, M. C., S. W. Bottjer, and A. P. Arnold (1984) Sexual dimorphism and lack of seasonal changes in vocal control regions of the white-crowned sparrow brain. Brain Res. *295:* 85–89.

Bottjer, S., E. Miesner, and A. P. Arnold (1984) Forebrain lesions disrupt development but not maintenance of song in passerine birds. Science *224:* 901–903.

Bottjer, S. W., J. N. Schoonmaker, and A. P. Arnold (1986) Auditory and hormonal stimulation interact to produce neural growth in adult canaries. J. Neurobiol. *17:* 605–612.

Canady, R. A. (1986) Doctoral dissertation, Rockefeller University.

Carlin, R. K., and P. Siekevitz (1983) Plasticity in the central nervous system: Do synapses divide? Proc. Natl. Acad. Sci. USA *80:* 3517–3521.

DeHoff, R. J., and F. N. Rhines (1961) Determination of number of particles per unit volume from measurements made on random plane sections: The general cylinder and the ellipsoid. Trans. Metallurgical Soc. Acad. of Metallurgical Eng. *221:* 975–982.

DeVoogd, T. J. (1986) Steroid interactions with structure and function of avian song control regions. J. Neurobiol. *17:* 177–201.

DeVoogd, T. J., and F. Nottebohm (1981a) Sex differences in dendritic morphology of a song control nucleus in the canary: A quantitative Golgi study. J. Comp. Neurol. *196:* 309–316.

DeVoogd, T. J., and F. Nottebohm (1981b) Gonadal hormones induce dendritic growth in the adult brain. Science *214:* 202–204.

DeVoogd, T. J., F. F. Chang, M. K. Floeter, M. J. Jencius, and W. T. Greenough (1981) Distortions induced in neuronal quantification by using camera lucida analysis: Comparisons using a semiautomated data acquisition system. J. Neurosci. Methods *3:* 285–294.

DeVoogd, T. J., B. Nixdorf, and F. Nottebohm (1985) Synaptogenesis and changes in synaptic morphology related to acquisition of a new behavior. Brain Res. *329:* 304–308.

Fairen, A., A. Peters, and J. Saldanha (1977) A new procedure for examining Golgi impregnation neurons by light and electron microscopy. J. Neurocytol. *6:* 311–337.

Freund, T. F., and P. Somogyi (1983) The section-Golgi impregnation procedure. I. Description of the method and its combination with histochemistry after intracellular iontophoresis or retrograde transport of horseradish peroxidase. Neuroscience *9:* 463–474.

Gottlieb, D. I., and W. M. Cowan (1972) On the distribution of axonal terminals containing spheroidal and flattened synaptic vesicles in the hippocampus and dentate gyrus of the rat and cat. Z. Zellforsch. Mikrosk. Anat. *129:* 413–429.

Hilman, D. E., and S. Chen (1985) Plasticity in the size of presynaptic and postsynaptic membrane specializations. In *Synaptic Plasticity,* C. W. Cotman, ed., pp. 39–76, Guilford, New York.

Kemp, J. M., and T. P. S. Powell (1971) The termination of fibers from the cerebral cortex and thalamus upon dendritic spines in the caudate nucleus: A study with the Golgi method. Phil. Trans. R. Soc. Lond. [Biol.] *262:* 429–439 (see also the preceding two articles by these authors in the same volume).

Konishi, M. (1965) The role of auditory feedback in the control of vocalization in the white-crowned sparrow. Z. Tierpsychol. *22:* 770–783.

Legan, S. J., G. A. Coon, and F. J. Karsch (1975) Role of estrogen as initiator of daily LH surges in the ovariectomized rat. Endocrinology *96:* 50.

Luine, V., F. Nottebohm, C. Harding, and B. S. McEwen (1980) Androgen affects cholinergic enzymes in songbird syringeal motorneurons and muscle. Brain Res. *192:* 89–107.

Marler, P. (1970) A comparative approach to vocal learning: Song development in white-crowned sparrows. J. Comp. Physiol. Psychol. *71:* 1–25.

Marler P., and M. S. Waser (1977) The role of auditory feedback in canary song development. J. Comp. Physiol. Psychol. *91:* 8–16.

Matsumoto, A., and Y. Arai (1979) Synaptogenic effect of estrogen on the hypothalamic arcuate nucleus of the adult female rat. Cell Tissue Res. *198:* 427–433.

Matus, A. I., and M. E. Dennison (1971) Autoradiographic localization of tritiated glycine at "flat vesicle" synapses in spinal cord. Brain Res. *32:* 195–197.

Nottebohm, F. (1980) Testosterone triggers growth of brain vocal control nuclei in adult female canaries. Brain Res. *189:* 429–436.

Nottebohm, F. (1981) A brain for all seasons: Cyclical anatomical changes in song control nuclei of the canary brain. Science *214:* 1368–1370.

Nottebohm, F., and A. P. Arnold (1976) Sexual dimorphism in vocal control areas of the songbird brain. Science *194:* 211–213.

Nottebohm, F., T. M. Stokes, and C. M. Leonard (1976) Central control of song in the canary, *Serinus canarius.* J. Comp. Neurol. *165:* 457–486.

Nottebohm, F., D. B. Kelley, and J. A. Paton (1982) Connections of vocal control nuclei in the canary telencephalon. J. Comp. Neurol. *207:* 344–357.

Nottebohm, F., M. Nottebohm, and L. A. Crane (1986) Developmental and seasonal changes in canary song and their relation to changes in the anatomy of song control nuclei. Behav. Neural Biol. *46:* 445–471.

Nottebohm, F., M. E. Nottebohm, L. A. Crane, and J. C. Wingfield (1987) Seasonal changes in gonadal hormone levels of adult male canaries and their relationship to song. Behav. Neural Biol. *47:* 197–211.

Pesch, A., and H-R. Güttinger (1985) Der Gesang des weiblichen Kanarienvogels. J. Ornithol. *126:* 108–110.

Peters, A., and M. L. Feldman (1976) The projection of the lateral geniculate nucleus to area 17 of the rat cerebral cortex. I. General description. J. Neurocytol. *5:* 63–84.

Shieh, J. Y., S. K. Leong, and W. C. Wong (1984) An electron microscopic study of the cerebellorubral connections after neonatal lesions in the sensorimotor and adjacent cortex in the albino rat. Brain Res. *324:* 1–10.

Stokes, T. C., C. M. Leonard, and F. Nottebohm (1974) A stereotaxic atlas of the telencephalon, diencephalon, and mesencephalon of the canary, *Serinus canarius.* J. Comp. Neurol. *156:* 337–374.

Thorpe, W. H. (1958) The learning of song patterns by birds, with special reference to the song of the chaffinch, *Fringilla coelebs.* Ibis *100:* 535–570.

Wann, D. F., T. A. Woolsey, M. L. Dierker, and W. M. Cowan (1973) An on-line digital-computer system for the semiautomatic analysis of Golgi-impregnated neurons. IEEE Trans. Biomed. Eng. *20:* 233–247.

Waser, M. S., and P. Marler (1977) Song learning in canaries. J. Comp. Physiol. Psychol. *91:* 1–7.

Williams, H., and F. Nottebohm (1985) Auditory responses in avian vocal motor neurons: A motor theory for song perception in birds. Science *229:* 279–282.

Wilson, C. J., P. M. Groves, S. T. Kitai, and J. C. Linder (1983) Three-dimensional structure of dendritic spines in the rat neostriatum. J. Neurosci. *3:* 383–398.